PCCP

Accepted Manuscript

ROYAL SOCIETY OF CHEMISTRY

www.rsc.org/pccp

Journal Name

RSCPublishing

ARTICLE

Towards a carbon independent and CO_2-free electrochemical membrane process for NH_3 synthesis

Cite this: DOI: 10.1039/x0xx00000x

K. Kugler, B. Ohs, M. Scholz and M. Wessling [a] *

Received 00th January 2012,
Accepted 00th January 2012

DOI: 10.1039/x0xx00000x

www.rsc.org/

Ammonia is exclusively synthesized by the Haber-Bosch process starting from precious carbon resources such as coal or CH_4. With H_2O, H_2 is produced and with N_2, NH_3 can be synthesized at high pressures and temperatures. Regrettably, the carbon is not incorporated into NH_3 but emitted as CO_2. Valuable carbon sources are consumed which could be used otherwise when carbon sources become scarce. We suggest an alternative process concept using an electrochemical membrane reactor (ecMR). A complete synthesis process with N_2 production and downstream product separation is presented and evaluated in a multi-scale model to quantify its energy consumption. A new micro-scale ecMR model integrates mass, species, heat and energy balances with electrochemical conversions allowing further integration into a macro-scale process flow sheet. For the anodic oxidation reaction H_2O was chosen as a ubiquitous H_2 source. Nitrogen was obtained by air separation which combines with protons from H_2O to NH_3 using a hypothetical catalyst recently suggested from DFT calculations. The energy demand of the whole electrochemical process is up to 20% lower than the Haber-Bosch process using coal as H_2 source. For the case of natural gas, the ecMR process is not competitive under today`s energy and resource conditions. In future however, the electrochemical NH_3 synthesis might be the technology-of-choice when coal is easily accessible over natural gas or limited carbon sources have to be used otherwise but for the synthesis of the carbon free product NH_3.

Introduction

Only recently, the direct NH_3 synthesis from its elements N_2 and H_2 has been considered one of the most significant scientific achievements of the 20th century[1]. The significance of NH_3 is self-evident: with 1-3% of the global energy consumption the NH_3 synthesis is one of the largest energy users in industry[2]. This is related to the energy intensive H_2 production, N_2 purification and the energy intensive process conditions to reach an acceptable conversion rate.

Today large-scale NH_3 manufacturing is carried out by the Haber-Bosch process operated at 400-500°C and 150-200 bars. The process parameters are a compromise between the thermal stability of NH_3, the catalyst activity and the reaction rate. At equilibrium a conversion of about 15% is obtained. The N_2 for the Haber-Bosch process is produced by air separation of liquid air[2]. The H_2 needed is mainly produced by steam reforming of hydrocarbons such as natural gas or coal at ~800°C. In total, the energy consumption of modern NH_3 plants is ~7.9 MWh/t_{NH3} using natural gas and ~13.5 MWh/t_{NH3} using coal as H_2 source[3]. The carbon is not incorporated into the final product NH_3, but emitted as CO_2[4]. From an environmental point of view, a NH_3 synthesis process avoiding CO_2-emissions and the consumption of precious carbon would be desirable. Additionally the direct N_2 fixation at ~100°C and ambient pressure could potentially reduce the energy demand compared to the Haber-Bosch process. An interesting application is the treatment of flue gas with NH_3, e.g. of ships and stationary facilities, to avert NO_x emissions. Hence, small-scale decentralized NH_3 synthesis plants conducted at ambient temperature and pressure are needed[5].

The operating pressure of the Haber-Bosch process is usually achieved by jet engine compressors, which work efficiently only at high flow rates. Hence, typical NH_3 production plants have capacities of at least 600 t_{NH3}/day[2]. The Haber-Bosch process has serious disadvantages, such as high energy consumption, environmental pollution such as CO_2-emission, and the thermodynamic limitation of the reaction. Up to now there is no other process economically competitive with the Haber-Bosch process.

A new process field is the electrochemical NH_3 synthesis. In 1996, Panagos et al. proposed a model to overcome the thermodynamic limitations of the reaction between N_2 and H_2 using a solid-state proton conductor which is placed between two electrodes[6]. Based on this model Marnellos and Stoukides reported an alternative route of NH_3 synthesis from its elements for the first time in 1998[7]. Since then, several studies on the

electrochemical NH_3 synthesis using molecular H_2 and N_2 have been reported. In these studies mainly Perovskite-, Pyrochlore- and Fluorite-type proton conductors have been used[8]. In 2000, Kordali et al. used water instead of molecular H_2 as proton source[9]. Thus the cost for H_2 production and purification do not apply. A Nafion membrane was used to divide the electrolytic cell in two half cells. The temperature could be reduced to 80-100°C resulting in a lower NH_3 decomposition and thus higher NH_3 yield.

Here, we propose the electrochemical synthesis in a membrane based process using an electrochemical membrane reactor (ecMR). A polymer proton exchange membrane (PEM) is used as proton conductive electrolyte. The PEM is sandwiched between the anodic and cathodic catalyst to form the membrane electrode assembly (MEA). A scheme of the two half-cell reactions occurring during the electrochemical NH_3 synthesis using a MEA is shown in Fig. 1:

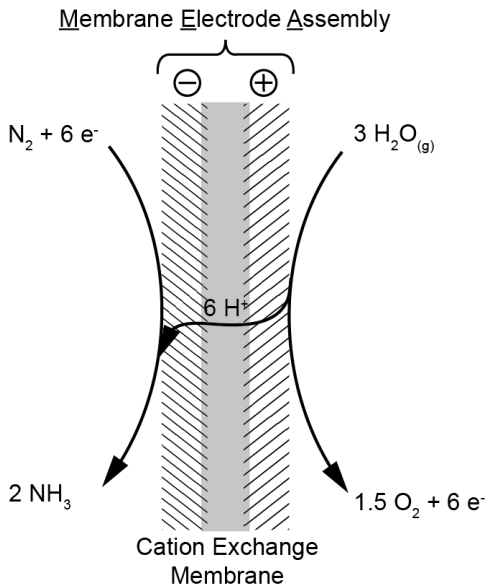

Figure 1 Suggested basic reactions for the electrochemical synthesis of NH_3 using a membrane electrode assembly (MEA) placed in a plate and frame stack-like electrochemical membrane reactor (ecMR).

The electrochemical synthesis of NH_3 can then be divided into two half-cell reactions:
Cathodic reduction of N_2:

$$N_2 + 6H^+ + 6e^- \rightarrow 2NH_3 (1)$$

Anodic oxidation of H_2O:

$$3H_2O \rightarrow 6H^+ + 6e^- + 1.5O_2 (2)$$

By applying an external potential to the ecMR, electrical energy is used as driving force for the otherwise non-spontaneous chemical reactions[10]. Ammonia is produced in a cathodic reaction, while the required protons are delivered by the oxidation of H_2O at the anode. This ecMR enables potentially a small-scale NH_3 production at low temperatures and pressures. In fact, Ruiquan and Gaochao could synthesize NH_3 at atmospheric pressure and 25-100°C and a potential of 2.5 V. Nafion102 and sulfonated polysulfone membranes prepared in laboratory were used as proton conductive membranes. The catalysts used were $Sm_{1.5}Sr_{0.5}NiO_4$ at the cathode and Ni-$Ce_{0.8}Sm_{0.2}O_{2-\delta}$ at the anode[11]. Just recently Lan et al. synthesized NH_3 from air and H_2O at ambient conditions. Pt/C was used at both electrodes as catalyst, separated by a Nafion211 membrane[12].

We present a multi-scale simulation model approach comprising two scales: (1) a microscopic model represents a new ecMR modeled using Aspen Custom Modeler (ACM). Mass and heat transport, species balances including chemical reactions and energy balances are solved. This complex ACM model can be integrated into (2) an overall macroscopic model using Aspen+ where all other unit operations are combined. A complete synthesis process with N_2 production and product separation downstream to the ecMR is then investigated. Our work aims to quantify whether such an electrochemical membrane based process is energetically favorable or competitive as compared to the Haber-Bosch process. The approach as well as the results serves as a role model to investigate future chemical process scenarios that go beyond a fossil based society.

Proposed Process

The entire synthesis process as shown in Fig. 2 was investigated using the process simulation program Aspen+.

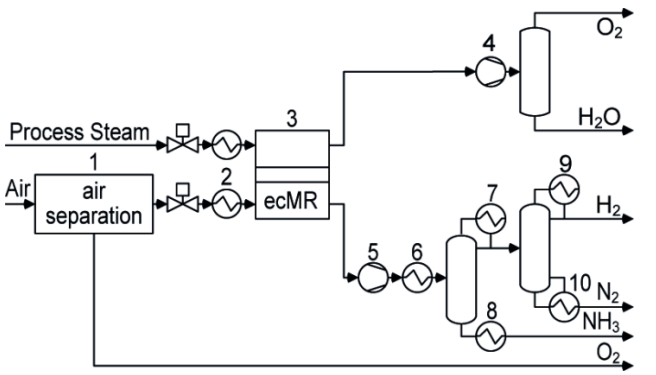

Figure 2 Flow diagram of the complete process modelled with Aspen Custom Modeller (ACM) including N_2 production by cryogenic air separation and product separation downstream to the ecMR.

The ecMR is a new user block modeled separately in ACM. Details of the complete set of energy and mass balances are described in the supporting information. The process model can be divided into three sections, namely feed pre-treatment, ecMR, and the anodic and cathodic product separation.

The first section is the feed pre-treatment. At the cathodic side this includes a cryogenic air separation which is not further optimized. The specific energy consumption is taken from literature[13]. The air separation is necessary to remove O_2 which otherwise would react with protons to H_2O and hence reduce the current efficiency. The rate determining step of the overall reaction in the ecMR is most likely one of the cathodic reaction

steps. Commonly N_2 leaves the cryogenic air separation unit at a pressure of 1.3-1.5 bar. At the cathode the amount of gas molecules increases during the reaction. Thus the N_2 pressure is reduced to atmospheric pressure before entering the reactor. To save costs the anodic feed is assumed to be conventional process steam. Depending on the steam available a pressure regulator has to be used and the steam has to be cooled. The ecMR of the process will be operated at 105°C (also compare Table 2).

The second section is the ecMR with the MEA as its core. The membrane acts as a gas diffusion and electron barrier to separate the anodic and cathodic half-cell. In each half-cell a serpentine flow channel is assumed to distribute the reactants on the catalyst layer of the MEA. An external power source delivers electrical current to the ecMR.

The third section is the product separation from unconverted feed gas to achieve a purity of 99.5% for each product. Oxygen, which is produced at the anode, is a by-product and can be sold to enhance the cost efficiency. Preliminary investigations have shown that simple condensation of H_2O in the anodic product stream is sufficient to obtain these purities. The cathodic product stream consists of NH_3, unconverted N_2 and H_2, which might be formed as side product at the cathode, depending on the current efficiency of the ecMR. In the Haber-Bosch process NH_3 is liquefied in a multi-stage condenser system. Since the product stream leaves the reactor at high pressure, H_2O can be used to liquefy NH_3 at room temperature. In general no further purification of NH_3 is necessary[2]. However, the ecMR is operated at lower pressure. Thus the product stream has to be pressurized and cooled in the separation unit. As a reference case two distillation columns are implemented in Aspen+ for the separation of the cathodic product stream. In the first column NH_3 is separated from H_2 and N_2. Subsequently N_2 and H_2 are separated in the second column. Although the energy demand of the product separation is significantly less compared to the ecMR, downstream processes and energy integration can be anticipated to reduce the overall energy demand. The results obtained here can serve as an upper estimate for the whole synthesis process and can give a first estimation of the energy consumption for a comparison with other processes.

Proposed ecMR

The modeled ecMR shown in Fig. 3 comprises seven functional elements.

The core is a polymeric membrane, which is laminated between the anodic and cathodic gas diffusion electrode (GDE). On top of these two electrodes the active catalyst layers (ACL) are located. Finally the two flow channels act as gas distributor and as electron distributor and collector at the cathode and the anode. Each half cell of the reactor can be exposed to different gases[14]. The electrocatalytic reactions take place at the three phase boundary (TPB) between fluid, membrane and one of the electrodes. A high catalytic surface area is required for an efficient process. The reactants are fed at the inlet of the reactor and flow through the flow channel where they get in contact with the GDE. The reactants diffuse through the electrodes to the ACL where the reactions take place. The products diffuse back to the flow channel and leave the reactor at the outlet.

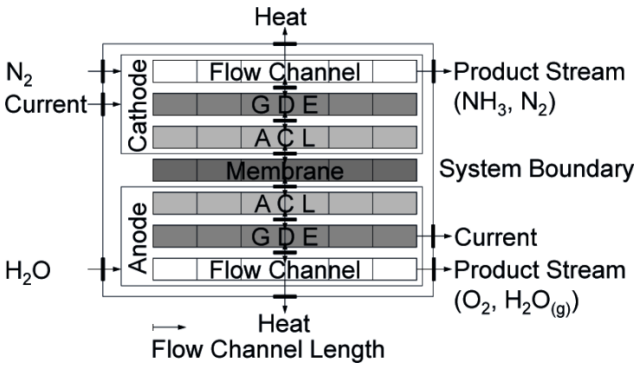

Figure 3 Main elements of the modeled ecMR and model discretization along the flow channel length in single elements (vertical dashed lines). Mass, heat and electron transfer to the surrounding.

Model structure of the ecMR

The model structure of the ecMR is illustrated in Fig. 3 as well. Heat is transferred to the ambient air through the outer walls of the cell. The electrons are supplied to and removed from the GDE. The cathode and anode consist of the flow channel, the GDE and the ACL. The flow channel and the GDE are connected through a boundary layer. Finally, a TPB layer connects the membrane with the ACL.

The heat and mass balance are calculated one dimensional along the flow channels. The concentrations in orthogonal direction to the flow channel, i.e. within the GDE and the ACL are calculated by linear mass transport relations. For this model the only assumed anodic reaction is the oxidation of H_2O to O_2 and protons. The reduction of N_2 to NH_3 and the formation of H_2 are the only cathodic reactions considered. Water crossover was neglected to keep the model simple. The ratio γ of the H_2 and NH_3 formation rate is given by Equ. (3):

$$\gamma = \frac{\dot{n}_{H_2}}{\dot{n}_{NH_3}} (3)$$

For the H_2 formation two electrons are required, while the NH_3 synthesis consumes three electrons. Hence, the current efficiency β of the cathode can be calculated as:

$$\beta = \frac{1}{1 + \frac{2}{3}\gamma} (4)$$

The model is implemented in ACM and consists of a set of parameters, variables and equations, which describe the physical and thermodynamically behavior. Therefore the flow channel is discretized along its length and is divided in incremental elements of the same length, as illustrated in Fig. 3 by the vertical dashed lines. Sufficient discretization steps were applied to achieve independency from the discretization. For the numerical solution ACM calculates the variables for each

element and the trend of each variable can then be examined along the domain. The proposed ecMR is modeled for a production capacity of ~1500 t/d, i.e. 19 m^2/t_{NH3} of flown through MEA area are needed.

Proposed catalyst

The protons for the cathodic reaction are delivered by an oxygen evolution reaction (OER) at the anode. The catalysts with the highest activity and the lowest overpotential for the OER are RuO_2 and IrO_2[15]. Many reaction mechanisms have been suggested and the electrochemical oxide path as well as the oxide path are widely accepted to occur for these catalysts[16]. For the N_2 reduction at the cathode four different reaction mechanisms are possible, namely both an associative and dissociative Tafel and Heyrovsky type mechanism[17]. Theoretical considerations showed that for most of the transition metals the dissociative mechanism occurs at lower voltages than the associative one. Furthermore, the activation barrier for the N_2 adsorption is relatively high for late transition metals[17].

The principle of Sabatier has widely been applied for the electrochemical H_2 production resulting in the so-called Volcano curve[18]. It allows estimating the activity of different catalysts[19]. Using Volcano plots Trasatti showed that the exchange current density j_0 of the hydrogen reaction on transition metals depends on the Gibbs free energy of adsorption of hydrogen atoms on the metal surface $\Delta G(M\text{-}H)$[20,21]:

$$\ln j_0 \sim \frac{\alpha \Delta G(M-H)}{k_B T} (5)$$

Recently, Skulason et al. evaluated theoretically possible transition metals as catalysts for the electrochemical NH_3 synthesis[17]. Using the density functional theory (DFT), they calculated the Gibbs free energy profile for the reduction of N_2. By assuming that the activation energy scales with the free energy difference in each elementary step, the catalytic activity has been investigated. The potential was calculated at which ΔG for each reaction step is smaller than or equal to zero to achieve significant reaction rates[17]. The resulting Volcano plot is given in Fig. 4.

The metals Mo, Fe and Rh have the highest activity for the electrochemical NH_3 synthesis. However, the metal surface will mainly be covered by *H as indicated by the white background and H_2 formation will be a competing reaction. In comparison Ti or Zr will mainly be covered by *N as indicated by the grey background and NH_3 will rather be synthesized than H_2. Hence, only early transition metals are promising catalysts for the electrochemical NH_3 synthesis.

For this work Ti-electrodes are considered because of their commercial availability and low price. Here an alternative synthesis process for NH_3 at mild reaction conditions, i.e. temperatures around 100°C and ambient pressure is investigated. Kordali et al. used a Ru cathode to synthesize NH_3 at ~90°C and 1 atm[9].

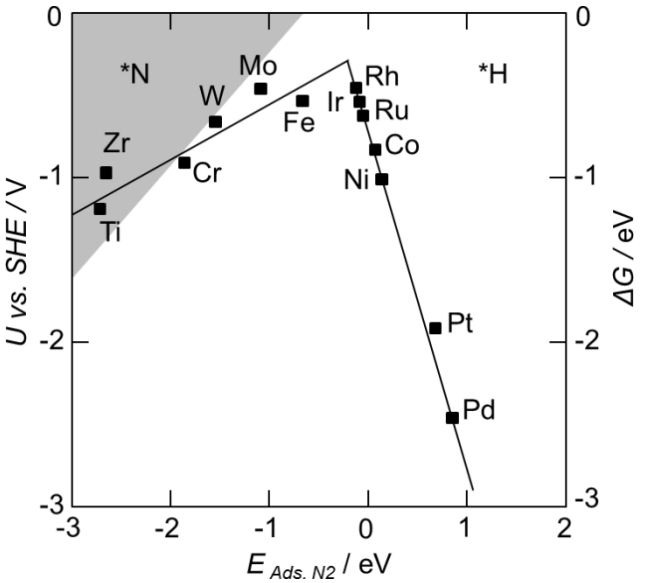

Figure 4 Volcano curve for the N_2 reduction (redrawn after[17]). Ti as hypothetical catalyst for electrochemical N_2 reduction at the cathode recently suggested from DFT calculations[17].

These reaction conditions are quite similar to the desired operating conditions of the proposed ecMR. The electrolytic cell of Kordali et al. is divided in two half-cells by placing a Nafion membrane between the anode and the cathode. Nitrogen was fed to the cathode, while an aqueous KOH solution was used as anodic electrolyte. At the anode an oxygen evolution reaction takes place. By applying a potential of -0.96 V a current density j of $1.2\text{x}10^{-6}$ A/cm^2 was obtained at an overpotential of 0.08 V. The conventional Butler-Volmer equation can be used to calculate the current exchange density j_0 of the Ru electrode. For the given conditions j_0 equals $5.5\text{x}10^{-10}$ A/cm^2.

The reaction mechanism for the N_2 reduction is assumed to be similar to the HER, namely a Heyrovsky- or Tafel-type reaction[17]. Thus, the dependencies for the hydrogen reaction, i.e. the Volcano curve and Equ. (5) might also be valid for the N_2 reduction. According to the Volcano curve the following equation is valid:

$$\frac{\partial(\log j_0)}{\partial\big(G(M-H)\big)} = r (6)$$

Since the NH_3 synthesis follows the same reaction mechanism, we assume the same slope r to be representative for the N_2 reduction. The dependency of j_0 on the adsorption energy and the results of Kordali et al. have been combined to estimate j_0 for Ti.

$$\log j_{0,Ti} = r\Delta\big(\Delta G(Ti-N) - \Delta G(Ru-N)\big) + \log j_{0,Ru} (7)$$

The NH_3 reaction rate increases with the applied current. However, a maximum for the reaction rate exists[8]. A further increase of the applied current does not result in a higher NH_3 reaction rate[22]. The electrode material and its catalytic activity have a significant influence on the reaction rate. Since some catalysts rather form H_2 than NH_3 the current efficiency depends on the catalyst material as well[8]. Based on the positive results of our study, we motivate more synthetic effort to tailor the catalysts to higher selectivity and productivity making the ecMR concept even more attractive. The cell potential has a similar impact on the NH_3 formation as the applied current. The reaction rate increases with the cell potential and a maximum exists above which the reaction rate is independent of the applied voltage[23]. For both low and high temperature applications the NH_3 reaction rate increases with temperature due to a higher protonic conductivity of the electrolytes[8]. However, an optimal temperature exists above which N_2 decomposes and the process efficiency gets reduced. For low temperature processes using polymer electrolytes, the ideal temperature depends on the H_2O content of the electrolyte and thus on the protonic conductivity.

Simulation results for the ecMR

The electrochemical membrane reactor (ecMR) is a user block modeled in Aspen Custom Modeler (ACM). Details of the complete set of energy and mass balances are described in the supporting information.

Reactor and process parameters

Important parameters such as the applied voltage or feed flow are changed within a specific range to find the optimal operating conditions of the ecMR. Reference values and the variation range are defined in Table 1.

Table 1. Reference parameters for the ecMR model

Parameter	Symbol	Value	Band	Unit
Current density	j	11	2 - 18	kA/m^2
Cell potential	U	2.20	2 - 2.325	V
Cathodic exchange current density	$j_{0,C}$	10^{-18}	10^{-35} - 10^{0}	A/m^2
Anodic feed flow rate	$\dot{V}_A$	180	120 - 240	ml/min
Cathodic feed flow rate	$\dot{V}_C$	60	40 - 80	ml/min
Current density	β	1	0.8 - 1	-

The overpotential and thus the cell voltage U are mainly influenced by the current density. Conventional ecMRs for H_2 production work at j ≈ 10 kA/m^2 [24]. A current density in this range is assumed to be optimal for the NH_3 synthesis as well, since the same electrolyte is used and the anodic reactions are equivalent. At the reference cell voltage of 2.2 V the current density is 11 kA/m^2. The lower bound for the cell voltage is 2 V since at lower values j is almost 0 kA/m² and a reasonable operation of the reactor is not possible. For the investigated ecMR almost all of the reactants are converted at a cell voltage of 2.325 V and a higher cell voltage would lower the energy efficiency of the process (also compare Fig. 8).

The exchange current density for a Ti-electrode has been estimated by combining theoretical calculations with experimental results for other electrodes. This theoretical consideration might not necessarily display the reality correctly. Accordingly, a wide band for j_0 has been examined to investigate its influence on the process performance.

The anodic and cathodic feed flow mainly influences the space-time-yield as well as the conversion rate. The conversion rate itself influences the energy demand for the separation units in the proposed process. The reference value for the anodic flow rate is three times higher than the cathodic one, since three times more H_2O than N_2 are converted to form NH_3.

At the chosen reference flow rates a conversion rate of ~50% is obtained. The upper bounds for the flow rates correlate to low conversion rates of ~35% for the given reference scenario. The lower bound for the flow rate corresponds to a conversion rate of ~80%. A further decrease of the flow rate would result in lower energy consumption for the separation units. The current efficiency β mainly influences the energy demand of the ecMR. For β = 1 no undesired parallel reactions such as H_2 formation are considered. At β = 0.8 the total energy demand of the suggested process is higher than for a coal based Haber-Bosch process. Thus in the variation range of 0.8 - 1.0 a comparison with the Haber-Bosch process is possible. Further parameters and important constants of the reactor model are listed in Table 2:

Table 2. Important parameters and constants of the model

Parameter	Symbol	Value	Unit
Anodic equilibrium potential [a]	E_A	1.17	V
Anodic exchange current density [b]	$j_{0,A}$	10^{-3}	A/m^2
Anodic charge transfer coefficient [b]	α_A	0.5	-
Number of transferred electrons anode [b]	$\nu_{e,A}$	2	-
Cathodic equilibrium potential [a]	E_C	-0.03	V
Cathodic charge transfer coefficient [c]	α_C	0.5	-
Number of transferred electrons cathode [b]	$\nu_{e,C}$	6	-
Membrane conductivity [d]	κ	17	A/Vm^2
Membrane thickness [d]	d_M	100	µm
GDE thickness [c]	d_{GDE}	200	µm
Ratio of catalytic surface area [a]	a_{CS}	5.3	m^2/m^2
Length flow channel [c]	l	0.9	m
Reactor temperature [c]	T^0	105	°C
Reactor pressure [c]	p	1	atm

[a] Calculated, [b] Taken from[25], [c] Assumed, [d] Taken from[26]

Performance indicators

For an energetic comparison of the ecMR with the Haber-Bosch process three different performance indicators are applied.

The first indicator is the specific energy consumption, which gives the energy consumed per ton synthesized product:

$$E_{spec} = \frac{U_{cell} \nu_e F}{\beta M_P \nu_P} \quad (8)$$

where M_P is the molar mass and ν_p the stoichiometric coefficient of the product.

The second indicator is the conversion rate of the reactants:

$$\zeta_{i,A/C} = \frac{\dot{n}_{\frac{A}{C},\alpha,i} - \dot{n}_{\frac{A}{C},\omega,i}}{\dot{n}_{\frac{A}{C},\alpha,i}} (9)$$

where $\dot{n}_{A/C,\alpha,i}$ is the molar flow rate of the reactant i at the inlet of the reactor and $\dot{n}_{A/C,\omega,i}$ at the outlet.

The third indicator is the energy efficiency, which is the ratio between the enthalpy of reaction and the consumed energy for the synthesis:

$$\eta = \frac{\Delta_R H}{U_{Cell} \nu_e F} (10)$$

System performance of the ecMR

Table 3 summarizes the simulation results for the performance indicators for the reference case.

Table 3. Results for the reference case

Parameter	Symbol	Value	Unit
Current density	j	11	kA/m^2
Cell potential	U	2.20	V
Specific energy consumption	E_{spec}	11.41	MWh/t
Energy efficiency	η	0.47	-
Conversion rate H_2O	ζ_{H2O}	0.53	-
Conversion rate N_2	ζ_{N2}	0.53	-
Mole fraction H_2O in anodic product stream	$y_{A,H2O}$	0.64	-
Mole fraction O_2 in anodic product stream	$y_{A,O2}$	0.36	-
Mole fraction N_2 in cathodic product stream	$y_{A,N2}$	0.69	-
Mole fraction NH_3 in cathodic product stream	$y_{A,NH3}$	0.31	-

The evolution of the current density along the flow channel for different cell voltages is given in Fig. 5.

The current density increases with increasing cell voltage. This is reasonable, as a higher cell voltage results in higher overpotentials for the electrochemical reactions. The current density decreases along the flow channel length, which can be explained considering the Gibbs free energy of the overall cell reaction $\Delta_R G$:

$$\Delta_R G = \Delta G^0 + RT \ln \left(\frac{\left(\frac{p_{O_2}}{p^0}\right)^{\frac{3}{2}} \left(\frac{p_{NH_3}}{p^0}\right)^2}{\left(\frac{p_{H_2O}}{p^0}\right)^3 \left(\frac{p_{N_2}}{p^0}\right)} \right) (11)$$

The concentration and the partial pressure of the reactants decrease along the flow channel, whereas the partial pressure of the products increases. Consequently $\Delta_R G$ increases and therefore the equilibrium potential of the cell increases as well. Otherwise the overpotential for the charge transfer has to decrease if the equilibrium potential decreases. This results in a lower current density along the flow channel length. This effect is more severe if a high cell voltage is applied. As the reaction rate increases with the cell voltage the conversion rate rises as well. Thus higher values for the second term on the right side of Equ. (11) occur.

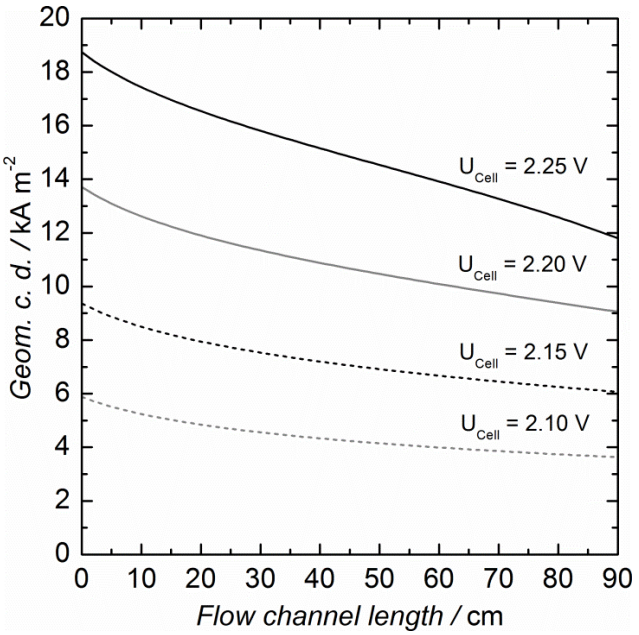

Figure 5 Evolution of the current density along the flow channel length for different cell voltages

The conversion rate of the reactants for the investigated ecMR is shown in Fig. 6.

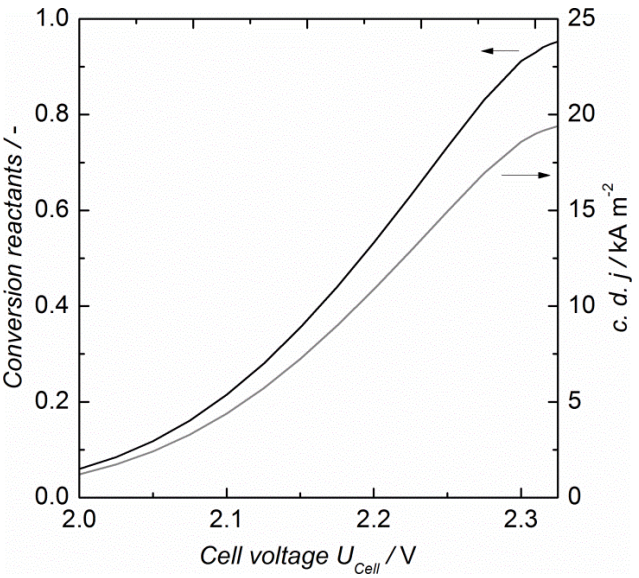

Figure 6 Influence of the cell voltage on the conversion rate and the average current density of the ecMR

At low cell voltages the conversion rate increases exponentially. The current density increases exponentially with the cell potential according to the Butler-Volmer equation. At higher cell voltages and thus higher current densities the effect

of Equ. (11) increases. Hence, j only increases linearly with the cell voltage. At very high cell voltages almost all of the reactants are converted and higher cell potentials cannot further increase the average current density and the conversion rate. Thus a minor dependency of the cell voltage on the average current density and conversion rate is observed at high cell potentials. Fig. 7 shows the evolution of the mole fractions along the flow channel. The slope of the mole fraction evolution decreases along the flow channel length due to the decreasing current density at the end of the reactor.

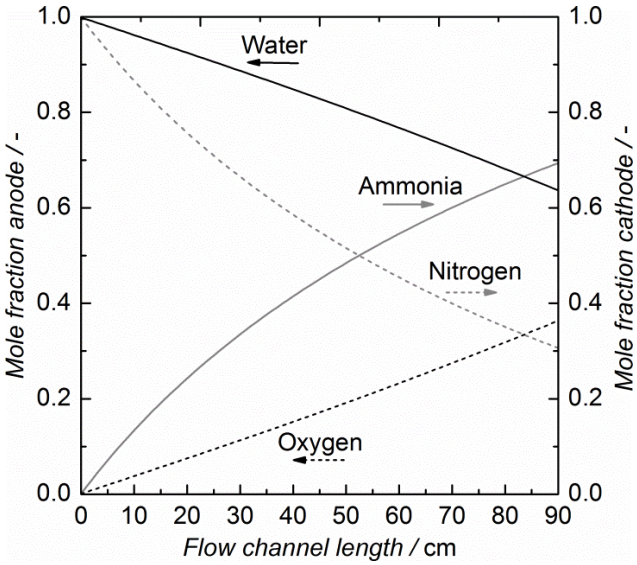

Figure 7 Evolution of the mole fraction in the anodic and cathodic flow channel

Different mole fractions at the anode and at the cathode are obtained for the same conversion rates of H_2O vapor and N_2. One reactant molecule forms two product molecules at the cathode, whereas two reactant molecules form only one product molecule at the anode.

The mole fractions at the outlets have main impact on the cost for the product separation. In Fig. 8 the achieved mole fractions for different cell voltages are shown. At the reference flow rates almost all of the reactants are converted at a cell voltage equal to or higher than 2.3 V.

The energy demand of the separation units are influenced by the volumetric feed flow rates at the anode and the cathode as well. At a fixed current density these parameters influence the conversion rates and thus the mole fractions at the outlet of the reactor. Besides that these parameters might influence the cell voltage which has to be applied to obtain the reference current density. To investigate this effect, one of the volumetric flow rates has been held constant whereas the other one has been varied. The results are given in Fig. 9.

The flow rate has only a minor influence on the cell voltage. Only at very low flow rates a higher cell voltage has to be applied since almost all of the reactants are converted. Thus the energy demand of the whole synthesis process can be reduced by decreasing the flow rate because at low flow rates very pure products are obtained. In Fig. 5 it was shown that the current density decreases along the flow channel, although the influence of the feed flow rate and thus of the conversion rate on the cell voltage is minor (see also Fig. 8).

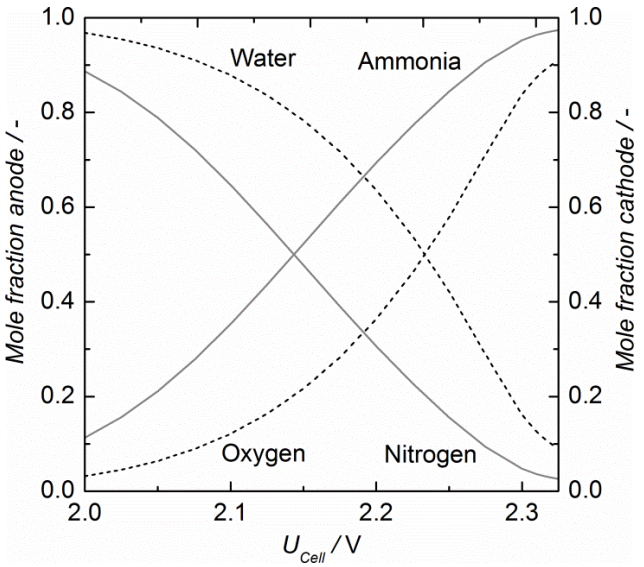

Figure 8 Mole fractions at the reactor outlets for different cell voltages

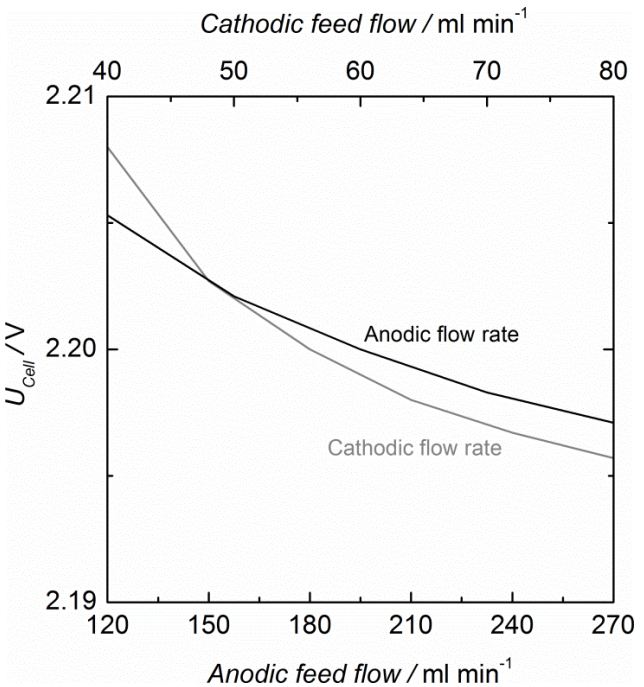

Figure 9 Cell potential which has to be applied to obtain the reference current density at different anodic and cathodic feed flow rates

To explain this, the influence of the mole fraction is considered. The difference of the equilibrium potential between a situation where the partial pressure of the reactants is 99% of the total pressure and a situation where the partial pressure of the products is 99% of the total pressure is 0.16 V. Obviously the composition has only a small impact on the equilibrium potential. However, it can be deduced that the reduction of the

overpotential for the charge transfer due to an increased equilibrium potential results in a higher decrease of the current density at higher overpotentials. Thus the decrease of the current density is higher at higher cell potentials (compare Fig. 5).

There are two possibilities to reduce the expenditure of the separation units: increase of the cell voltage or decrease of the flow rate. An increase of the cell voltage leads to higher operation costs whereas a lower flow rate decreases the space-time yield. A lower space-time yield generally increases the investment costs for the reactor. Hence, there will be a trade-off between the energy consumption for the separation units, the energy-consumption of the reactor and the investment costs.

So far there has been no experimental investigation about the reaction kinetics of the electrochemical nitrogen reduction on early transition metals. Therefore the exchange current density has been estimated combining the theoretical calculations of Skulason et al. and the experimental results of Kordali et al. for a Ru cathode[17,9]. However, the exchange current density obtained from this consideration might not be exact. The influence of this parameter on the process performance has been investigated as well, which is shown in Fig. 10.

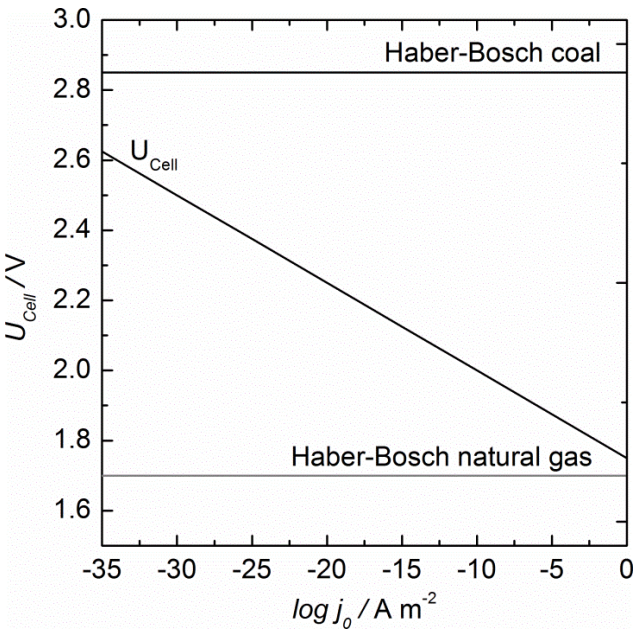

Figure 10 Cell voltage for different exchange current densities at a given current density. The horizontal lines represent the cell potential which can be applied so that the energy consumption of the ecMR equals different Haber-Bosch processes

The cell voltage which has to be applied for a given current density of 11 kA/m^2 is plotted against the logarithmic exchange current density of the cathodic reaction. A linear curve is obtained which is reasonable as the overpotential is a linear function of the logarithm of the exchange current density and of the logarithm of the current density, which has been hold constant, as well. Equ. (8) allows the calculation of the energy consumption for the ecMR. Based on this equation the cell voltage which can be applied to equal the energy consumption of the ecMR with the energy demand of conventional NH_3 synthesis plants can be determined. The cell voltages representing conventional Haber-Bosch plants are given by two horizontal lines in Fig. 10. The upper one corresponds to the Haber-Bosch process using coal as H_2 source, whereas the lower one belongs to the Haber-Bosch process using natural gas. For this consideration neither the energy for the product separation nor for the feed pre-treatment are taken into account yet. However, even if the exchange current density for the cathodic reaction is very high, the electrochemical process cannot compete in terms of energy consumption with the natural gas based Haber-Bosch process. But even at very low exchange current densities the energy consumption will be lower than for a Haber-Bosch process using coal as feedstock for H_2 production.

To investigate potentials for the process improvement, the different potential drops within the reactor are plotted for different current densities in Fig. 11.

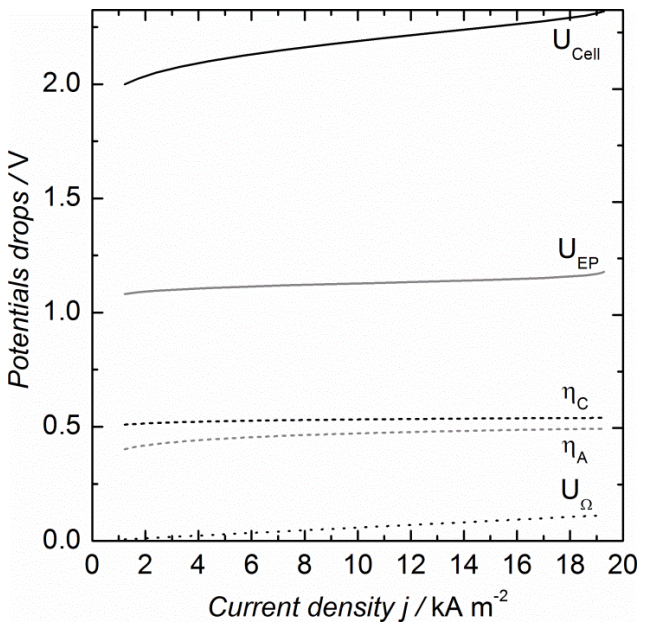

Figure 11 Cell voltage and overpotentials of the electrochemical membrane reactor for different current densities

The equilibrium potential is the main contributor to the cell voltage. This value cannot be changed as it is determined by thermodynamics. Further main contributors are the cathodic and anodic overpotentials to drive the charge transfers. The overpotential for the cathodic reaction is higher which relates to the low activity of the cathodic reaction and thus to the very low exchange current density. Hence, this gives the highest potential to improve the process performance. The overpotential at the anode is lower, but it is worthwhile to search for better catalyst at the anode. The ohmic potential loss increases linear with the current densities. Thus for high current densities this contribution cannot be neglected.

At the cathode H_2 formation is a competing reaction for the NH_3 synthesis. So far a current efficiency of unity, which

means that no H_2 is produced, was assumed because it is expected that on Ti-electrodes mainly NH_3 is produced[17]. However, these assumptions are based on theoretical considerations taking the binding energy of N_2 and H_2 on the electrode surface into account. In this work the influence of the current efficiency on the specific energy consumption as well as on the composition of the product stream are investigated (compare Fig. 12).

The energy consumption per ton product in kWh/t_{NH3} can be calculated as following[27]:

$$E_{spec} = \frac{U_{cell} v_e}{3.6 \beta M_{NH3} v_{NH3}} \quad (12)$$

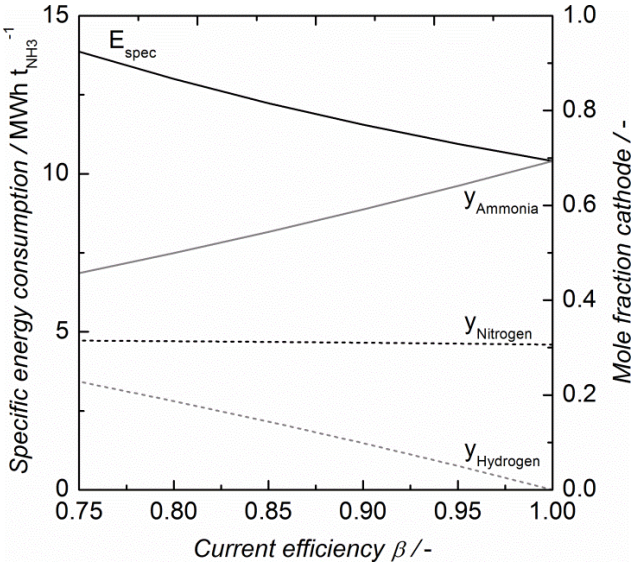

Figure 12 Influence of the current efficiency on the specific energy consumption and on the molar composition of the product stream at the cathode

At a current efficiency of unity 10.4 MWh/t_{NH3} are consumed at the reference cell voltage. This value increases up to 13.0 MWh/t_{NH3} for a current efficiency of at least 80%. As mentioned before, there are no experimental results concerning the current efficiency available. However, it is expected that the current efficiency is relatively high because N_2 atoms bind more strongly than H_2 on the Ti-surface. Hence, the electrode will mainly be covered by N_2 and NH_3 will be formed more probably[17]. Accordingly, a current efficiency of 80% seems to be reasonable. A lower current efficiency does not only increase the specific energy consumption of the reactor, but also the separation is more complex and particularly the H_2/N_2 separation is energy intensive. For the investigated current efficiencies the molar H_2 fraction in the cathodic product stream varies between 0 and approximately 20%.

Process energetics

The multi-scale modeling presented above allows answering the question if the electrochemical membrane based process is energetically favorable or competitive as compared to the Haber-Bosch process. To answer this question the discussed reference case and four different cases shown in Table 4 are considered.

The influence of different parameters on the energy consumption of the model process is investigated. These cases have been chosen arbitrarily, however, they can indicate how different process parameters influence the energy consumption of the separation units.

Table 4. Five different case conditions to investigate the energy demand of the model process

Case	explanation	U_{cell} [V]	current efficiency [-]
1	reference case	2.20	1.0
2	high cell voltage	2.25	1.0
3	low cell voltage	2.15	1.0
4	medium current efficiency	2.20	0.9
5	low current efficiency	2.20	0.8

The energy consumption per ton produced NH_3 of the different process units as numbered in Fig. 2 are listed in Table 5.

Table 5. Energy demand of the entire synthesis process in MWh/t_{NH3}

Process unit	Case 1	Case 2	Case 3	Case 4	Case 5
Cryogenic air separation (1)	0.08	0.08	0.08	0.08	0.08
Heat exchanger (2)	0.04	0.03	0.06	0.04	0.04
ecMR (3)	10.40	10.63	10.16	11.50	13.00
Compressor (4)	0.26	0.13	0.34	0.30	0.24
Compressor (5)	0.31	0.25	0.40	0.36	0.43
Heat exchanger (6)	0.07	0.06	0.11	0.09	0.11
Condenser (7)	0.14	0.06	0.36	0.26	0.35
Reboiler (8)	0.11	0.12	0.08	0.13	0.12
Condenser (9)	-	-	-	0.12	0.13
Reboiler (10)	-	-	-	0.03	0.03
Sum	11.41	11.36	12.60	12.93	14.55

With 11.36 MWh/t_{NH3} the lowest energy demand for the entire process is achieved in case 2. In comparison to cases 1 and 3 the total energy demand is lower, since the energy demand for the separation units is much lower. At lower cell voltages and fixed flow rates the conversion rate is lower and much more flow volume has to be separated per ton NH_3. Additionally, the ecMR has the by far highest contribution to the total energy demand for the process.

Table 6 compares the ecMR with the Haber-Bosch process: the energy demand for the ecMR in case 2 is 3.46 MWh/t_{NH3} higher than for the Haber-Bosch process using natural gas as H_2 source.

Table 6. Energy demand of different process alternatives in MWh/t_{NH3} *

Haber-Bosch natural gas	Haber-Bosch coal	ecMR U_{cell} = 2.25V
7.92	13.47	11.36

* Values for Haber-Bosch are taken from[4]

However, if other H_2 sources such as coal are used the energy demand of the Haber-Bosch process almost doubles[3] and the suggested ecMR scenario becomes energy-wise viable. A comparison between the energy demands for cases 4 and 5 and

for the coal based Haber-Bosch process leads to a minimum current efficiency for the ecMR of 87% to be competitive.

Conclusion

Since the conceptual ecMR can be installed in decentralized small-scale plants, the electrical energy can be delivered from local renewable energy sources such as wind or hydro-power. Additionally the electrochemical synthesis has several other advantages. The ecMR can be operated at lower temperature and pressure and thus the investment costs might be lower. Besides that smaller and more flexible plants can be used. In comparison, Haber-Bosch plants just work efficiently at very high capacities. In addition, the Haber-Bosch process uses valuable carbon-based feedstock such as natural gas, heavy hydrocarbons or coal, whereas the electrochemical process uses easily accessible process steam and air. Since H_2O is used as proton source, no CO_2-emissions will occur due to H_2 production. The catalytic activity of the electrodes, which result in a higher j_0 and thus lower overpotential for the charge transfer, shows the highest potential for improvements. Additionally, the separation processes can be improved significantly. Using current data from DFT simulations and applying a new microscopic reactor model integrated into a macroscopic process flow sheet we substantiate possible scenarios towards new process alternatives for the current Haber-Bosch process. Most likely such processes will be of electrochemical nature; whether or not the electrochemical reactor proposed here will be the final choice is irrelevant. Essential is the proposed multi-scale approach of quantum chemical and molecular simulations with a microscopic reactor model integrated into a overall chemical process.

Notes and references

[a] K. Kugler, B. Ohs, M. Scholz, Prof. M. Wessling
Aachener Verfahrenstechnik - Chemical Process Engineering
RWTH Aachen University
Turmstr. 46, 52064 Aachen, Germany
[*] Prof. M. Wessling
Aachener Verfahrenstechnik - Chemical Process Engineering
RWTH Aachen University
Turmstr. 46, 52064 Aachen
E-mail: manuscripts.cvt@avt.rwth-aachen.de

Electronic Supplementary Information (ESI) available: Details of the complete set of energy and mass balances. See DOI: 10.1039/b000000x/

1. V. Smil, *Nature*, 1999, **400**, 415.
2. M. Appl, in *Ullmann's Encyclopedia of Industrial Chemistry, Ammonia*, Wiley-VCH Verlag GmbH & Co. KGaA, Weinheim, 2006.
3. M. Appl, in *50th Anniversary of the IFA Technical Conference September 25-26th 1997, Sevilla, Spain*, 1997.
4. J. Hagen, *Industrial Catalysis*, Wiley-VCH Verlag GmbH & Co. KGaA, Weinheim, 2006.
5. R. M. Heck, *Catal. Today*, 1999, **53**, 519–523.
6. E. Panagos, I. Voudouris, and M. Stoukides, *Chem. Eng. Sci.*, 1996, **51**, 3175–3180.
7. G. Marnellos and M. Stoukides, *Science*, 1998, **282**, 98–100.
8. I. A. Amar, R. Lan, C. T. G. Petit, and S. Tao, *J Solid State Electrochem*, 2011, **15**, 1845–1860.
9. V. Kordali, G. Kyriacou, and C. Lambrou, *Chem Commun*, 2000, 1673–1674.
10. M. Stoukides, *Catal Rev*, 2000, **42**, 1–70.
11. R. Liu and G. Xu, *Chin. J. Chem.*, 2010, **28**, 139–142.
12. R. Lan, J. T. S. Irvine, and S. Tao, *Sci. Rep.*, 2013, **3**, 1145–1145.
13. M. Appl, *Ammonia: Principles and Industrial Practice*, Wiley-VCH Verlag GmbH, Weinheim, 1999.
14. G. Marnellos and M. Stoukides, *Solid State Ionics*, 2004, **175**, 597–603.
15. K. Kinoshita, *Electrochemical Oxygen Technology*, John Wiley & Sons,Inc., 1992.
16. J. O. Bockris, *J. Chem. Phys.*, 1956, **24**, 817–827.
17. E. Skúlason, T. Bligaard, S. Gudmundsdóttir, F. Studt, J. Rossmeisl, F. Abild-Pedersen, T. Vegge, H. Jónsson, and J. K. Nørskov, *Phys. Chem. Chem. Phys.*, 2012, **14**, 1235–1245.
18. H. Wendt and G. Kreysa, *Electrochemical Engineering: Science and Technology in Chemical and Other Industries*, Springer-Verlag Berlin Heidelberg, 1999.
19. M. M. Jaksic, *J New Mat Elect Syst*, 2000, **3**, 167–182.
20. S. Trasatti, *Z Phys Chem Neue Fol*, 1975, **98**, 75–94.
21. E. Santos and W. Schmickler, *Catalysis in Electrochemistry: From Fundamentals to Strategies for Fuel Cell Development*, John Wiley & Sons, Inc., 2011.
22. Y. Guo, B. Liu, Q. Yang, C. Chen, W. Wang, and G. Ma, *Electrochem Commun*, 2009, **11**, 153–156.
23. Z.-J. Li, R.-Q. Liu, J.-D. Wang, Y.-H. Xie, and F. Yue, *J Solid State Chem*, 2005, **9**, 201–204.
24. H. Wendt, H. Vogt, G. Kreysa, D. M. Kolb, G. E. Engelmann, J. C. Ziegler, H. Goldacker, K. Jüttner, U. Galla, H. Schmieder, and E. Steckhan, in *Ullmann's Encyclopedia of Industrial Chemistry, Electrochemistry*, Wiley-VCH Verlag GmbH & Co. KGaA, Weinheim, 2009.

25. P. Choi, D. G. Bessarabov, and R. Datta, *Solid State Ionics*, 2004, **175**, 535–539.

26. S. Slade, S. a. Campbell, T. R. Ralph, and F. C. Walsh, *J Electrochem Soc*, 2002, **149**, A1556–A1564.

27. V. Schmidt, *Elektrochemische Verfahrenstechnik*, Wiley-VCH Verlag GmbH & KGaA, Weinheim, 2003.

A new NH_3 synthesis process using an electrochemical membrane reactor including N_2 production and product separation is modelled in Aspen+.